Atmos. Chem. Phys. Discuss., 13, 24855–24884, 2013
www.atmos-chem-phys-discuss.net/13/24855/2013/
doi:10.5194/acpd-13-24855-2013

Atmospheric Chemistry and Physics
Open Access
Discussions

Heterogeneous reaction of N_2O_5 with illite and Arizona Test Dust particles

M. J. Tang, G. Schuster, and J. N. Crowley

Department of Atmospheric Chemistry, Max Planck Institute for Chemistry, Hahn-Meitner-Weg 1, 55128 Mainz, Germany

Received: 6 September 2013 – Accepted: 9 September 2013 – Published: 24 September 2013

Correspondence to: J. N. Crowley (john.crowley@mpic.de)

Published by Copernicus Publications on behalf of the European Geosciences Union.

Abstract

The heterogeneous reaction of N_2O_5 with airborne illite and Arizona Test Dust particles was investigated at room temperature and at different relative humidities using an atmospheric pressure aerosol flow tube. N_2O_5 at concentrations in the range 8 to 24×10^{12} molecule cm^{-3} was monitored using thermal-dissociation cavity ring-down spectroscopy at 662 nm. At zero relative humidity a large uptake coefficient of N_2O_5 to illite was obtained, $\gamma(N_2O_5) = 0.09$, which decreased to 0.04 as relative humidity was increased to 67 %. In contrast, the uptake coefficient derived for ATD is much lower (∼ 0.006) and, within experimental uncertainty, independent of relative humidity (0–67 %). Potential explanations are given for the significant differences between the uptake behaviour for ATD and illite and the results are compared with uptake coefficients for N_2O_5 on other mineral surfaces.

1 Introduction

Mineral dust particles, lifted into the atmosphere from arid and semi-arid regions with a global annual flux of ∼ 2000 Tg (Textor et al., 2006), can impact direct radiative forcing by scattering and absorbing solar radiation (Balkanski et al., 2007) and also modify indirect radiative forcing by serving as cloud condensation nuclei (Twohy et al., 2009) and ice nuclei (DeMott et al., 2003; Klein et al., 2010). After being mobilized, dust particles with a mass mean diameter of < 10 µm can stay in the troposphere for a few days and be transported over thousands of kilometres (Prospero, 1999; Fairlie et al., 2010). The heterogeneous reactions of mineral dust particles during transport can directly and/or indirectly impact the levels of many important trace gases, including NO_x, O_3, and HO_x radicals (Dentener et al., 1996; de Reus et al., 2005; Wang et al., 2012; Zhu et al., 2010). In addition, the chemical aging of dust particles (e.g. formation of particulate nitrate and/or sulphate) (Laskin et al., 2005; Matsuki et al., 2005; Mori et al., 2003; Sullivan et al., 2007) can modify their hygroscopicity and ability to serve as cloud condensation nuclei (Krueger et al., 2003; Shi et al., 2008; Sullivan et al., 2009; Tobo et al., 2010). Finally, heterogeneous processing can influence the ice nucleation properties of mineral dust particles (Cziczo et al., 2009; Kanji et al., 2013; Niedermeier et al., 2010; Sullivan et al., 2010).

N_2O_5 is formed in the reaction of NO_2 with NO_3 radicals, the latter formed by the oxidation of NO_2 by O_3 (R1) (Wayne et al., 1991). N_2O_5 thermally decomposes back to NO_2 and NO_3 radicals, leading to a dynamic equilibrium between NO_2, NO_3, and N_2O_5 (R2) which is usually achieved within a few minutes under most conditions in the lower atmosphere (Crowley et al., 2010b; Osthoff et al., 2007).

$$NO_2 + O_3 \rightarrow NO_3 + O_2 \tag{R1}$$

$$NO_2 + NO_3 + M \leftrightarrow N_2O_5 + M \tag{R2}$$

N_2O_5 plays a significant role in tropospheric chemistry by contributing to the removal of NO_x and the formation of particulate nitrate (Dentener and Crutzen, 1993; Evans and Jacob, 2005; Brown et al., 2006) as well as heterogeneous chlorine activation through the formation of $ClNO_2$, e.g. (Osthoff et al., 2008; Thornton et al., 2010; Phillips et al., 2012). The atmospheric NO_x and O_3 burdens are sensitive to the variation of $\gamma(N_2O_5)$ in the range of 0.001–0.02 (Macintyre and Evans, 2010). In general N_2O_5 is only important during the night-time because NO_3 radicals (precursor and equilibrium partner) are rapidly photolysed and react with NO during the day (Wayne et al., 1991).

The uptake of N_2O_5 onto mineral dust particles has been investigated using bulk dust samples in a Knudsen reactor (Seisel et al., 2005; Karagulian et al., 2006; Wagner et al., 2008), airborne particles in an aerosol chamber (Mogili et al., 2006a) and in an aerosol flow tube (Wagner et al., 2008, 2009). Recently, aerosol flow tubes with detection of N_2O_5 by cavity ring-down spectroscopy were deployed to study the reaction of N_2O_5 with Saharan dust aerosol (Tang et al., 2012). The same apparatus has

ACPD
13, 24855–24884, 2013

been used in this study to investigate the heterogeneous uptake of N_2O_5 onto airborne Arizona Test Dust (ATD) and illite particles.

In order to assess the atmospheric importance of the uptake of N_2O_5 to mineral dust accurately, it is necessary to understand how strongly this parameter is correlated with the composition (mineralogy) of the dust particles. One might, for instance expect that, being a di-acid anhydride, N_2O_5 uptake will be favoured on particles which are alkaline and/or which have a high affinity to water, so that the efficiency of uptake would be enhanced at high relative humidity (RH).

To date, the database of reliable measurements of N_2O_5 uptake at atmospherically relevant RH is very small and the conclusions appear counter intuitive, with both positive and negative impacts on the uptake coefficient reported for increases in RH. For example, the uptake coefficient of N_2O_5, $\gamma(N_2O_5)$, onto quartz is reported to be enhanced by a factor of 4 when increasing RH from 0 % to 43 % RH (Mogili et al., 2006a). Similarly, for $CaCO_3$, $\gamma(N_2O_5)$ increased from $(4.8 \pm 0.7) \times 10^{-3}$ at 0 % RH to $(19.4 \pm 2.2) \times 10^{-3}$ at 71 % RH (Wagner et al., 2009).

In contrast, $\gamma(N_2O_5)$ on Saharan dust particles showed no dependence (Tang et al., 2012) or slightly negative dependence (Wagner et al., 2008) on RH. Previous aerosol flow tube studies of the uptake of N_2O_5 onto quartz and ATD were only carried out at two different relative humidities (0 % and 29 %) (Wagner et al., 2009) and no definite conclusions regarding the effect of RH could be made.

We extend this database by investigating the effects of relative humidity on the uptake of N_2O_5 to illite, one of the most abundant clay minerals in dust particles (Chester, 1990; Claquin et al., 1999; Nickovic et al., 2012) and one of the most efficient ice nuclei in the troposphere (Eastwood et al., 2008; Zimmermann et al., 2008). Illite, with the general formula $M_x[Si_{6.8}Al_{1.12}]Al_3Fe_{0.25}Mg_{0.75}O_{20}(OH)_4$ (where M is a monovalent interlamellar cation), is a non-expansive clay mineral characterized by aluminosilicate layers containing one octahedral alumina sheet sandwiched by two tetrahedral silica sheets (Hatch et al., 2012). At room temperature one monolayer of surface-adsorbed water is formed at ~ 15 % RH (Hatch et al., 2012), and the amount of adsorbed water

Discussion Paper | Discussion Paper | Discussion Paper | Discussion Paper |

ACPD

13, 24855–24884, 2013

Heterogeneous reaction of N_2O_5

M. J. Tang et al.

increases to 0.15–0.2 g water per gram illite (corresponding to ~60–80 formal monolayers of water) at ~70 % RH (Schuttlefield et al., 2007; Hatch et al., 2012). For comparison, we have also investigated the uptake of N_2O_5 to ATD, which is essentially ground sand from the Arizona desert and which, although possessing a mineralogy that does not correspond closely to that of globally important sources of atmospheric mineral dust aerosols, e.g. Saharan or Asian dust, has often been used as a laboratory surrogate for investigations of heterogeneous reactivity (Crowley et al., 2010a) and cloud nucleation efficiency of mineral dust particles (Sullivan et al., 2010; Vlasenko et al., 2005). Though the uptake of N_2O_5 onto mineral dust particles has been confirmed to lead to the formation of particulate nitrate (Seisel et al., 2005; Tang et al., 2012), it is still not clear why different mineral dust components shows variable heterogeneous reactivity towards N_2O_5 (Crowley et al., 2010a). Investigation of the uptake of N_2O_5 onto different dust components can shed light on the reaction mechanisms, and e.g. indicate which factors control the rate of heterogeneous reaction of N_2O_5.

2 Experimental

The heterogeneous reaction of N_2O_5 with airborne ATD and illite particles was investigated using an aerosol flow tube (AFT) operated at room temperature and atmospheric pressure of N_2.

2.1 Aerosol flow tube

A schematic diagram of the experimental set-up is given in Fig. 1. The flow tube is a vertically-mounted Pyrex tube with a length of 120 cm and an inner diameter of 4.1 cm. A flow ($F_A + F_B + F_D$) of 2800 cm^3 (STP) min^{-1} (sccm) containing dispersed illite or ATD was introduced into the top of the flow tube via the side arm. Gaseous N_2O_5 was eluted from a crystalline sample held at 223–233 K with a small N_2 flow (F_K, 10–40 sccm) and diluted by F_C to a total flow of 200 sccm. This flow was then transported through a 1/8″

Discussion Paper | Discussion Paper | Discussion Paper | Discussion Paper |

ACPD
13, 24855–24884, 2013

Heterogeneous reaction of N_2O_5

M. J. Tang et al.

Title Page
Abstract Introduction
Conclusions References
Tables Figures
◀| |▶
◀ ▶
Back Close
Full Screen / Esc

Printer-friendly Version
Interactive Discussion

PFA tube (inner diameter: ~ 1.5 mm) into the lower 10 cm of the stainless steel injector (inner diameter: 5 mm) and then into the centre of the AFT. The inner wall of the lower 10 cm of the injector was coated with Teflon (FEP) to reduce the loss of N_2O_5. Another small flow (F_E, 10 sccm) was used to purge the annular space between the injector and the 1/8″ Teflon tube. The position of the injector could be adjusted to vary the interaction time between N_2O_5 and dust aerosols. The total flow through the reaction volume was typically 3010 sccm, resulting in a linear flow velocity of ~ 4.2 cm s^{-1} and a Reynolds number of 112, indicating that the flow is laminar with an entrance length of ~ 26 cm required to fully develop the laminar flow. The mixing length was calculated to be ~ 42 cm (i.e. a mixing time of ~ 10 s) (Keyser, 1984), using a diffusion coefficient of 0.085 cm^2 s^{-1} for the diffusion of N_2O_5 in N_2 at atmospheric pressure (Wagner et al., 2008).

The wall of the flow tube was kept dusty and therefore highly reactive towards N_2O_5. In this case the loss of N_2O_5 onto the wall was close to being gas phase diffusion limited and was thus largely independent of fluctuations in the wall loss rate constant caused e.g. by variations of the dust particle concentration in the AFT. Measurement of the N_2O_5 wall loss rates before and after the uptake experiments confirmed that the loss of N_2O_5 onto the wall of the flow tube was limited by gas phase diffusion.

2.2 Dust aerosol generation and characterization

The illite sample was obtained from the Source Clay Minerals Repository, University of Missouri, Columbia, USA. Arizona Test Dust particles (nominal 0–10 µm) were purchased from Powder Technology Inc., Burnsville, MN, USA. Dispersed illite samples were generated using a commercially available Rotating Brush Generator (RBG), and then entrained into an 800 sccm flow (F_D). ATD samples were dispersed using a self-built aerosol generator as described in Wagner et al., (2009). The aerosol flow was diluted by the carrier gas ($F_A + F_B$, 2000 sccm) to a total flow of 2800 sccm, transported through a 1/4" aluminium tube, and delivered into the reaction volume via the side arm. The ratio of F_A to F_B could be varied in order to adjust the relative humidity up to 67 %.

ACPD
13, 24855–24884, 2013

Before being diluted by the carrier gas, the aerosol flow (800 sccm) was delivered into a 5 L glass vessel (with a residence time of 6–7 min) to smooth out any spikes in the dust aerosol concentration.

At the bottom of the flow tube, particle-free air was added to increase the total flow to 5 L min^{-1} prior to further dilution by a factor of 20 using a TSI 3302A aerosol dilutor, and measurement by a TSI 3321 Aerodynamic Particle Sizer (APS). The APS provided both the size distribution and an analogue output proportional to the aerosol number concentration and which was synchronized to the N_2O_5 signals. The APS measures the time of flight of a particle over a fixed distance to derive the equivalent aerodynamic diameter, D_a, which is the diameter of the spherical particle of unity density with the identical aerodynamic properties of the dust particle under investigation (Hinds, 1996). If the density of the particle, ρ, is known, the equivalent Stokes diameter can be derived:

$$D_s = \frac{D_a}{\sqrt{\rho}} \quad (1)$$

In this study, the density for both ATD and illite particles was assumed to be 2.7 g cm^{-3}. The same density was used for ATD in a previous study (Wagner et al., 2009). In order to take into account the non-sphericity of dust particles, a shape factor of 1.36 has been proposed (Hinds, 1996). In a previous study, (Wagner et al., 2008) compared the time-integrated particle mass with size-resolved particle number concentration measurement using an APS and derived a correction factor of 1.6. These considerations lead us to conclude that the surface area of the dust particles might be overestimated (and thus the uptake coefficient underestimated) by a factor of up to ∼ 2.

The aerodynamic size distributions of illite and ATD are displayed in Fig. 2. The average surface area (weighted per pin), calculated using the Stokes diameters, is 21.1 µm^2 per particle for ATD and 3.56 µm^2 per particle for illite. No significant change in particle size distribution occurred over the course of an experiment (∼ 1 h) for either ATD or illite.

2.3 N_2O_5 generation and detection

Crystalline N_2O_5 was synthesized by reacting NO_2 with excess O_3 in a glass reactor and trapping the product in a cold finger kept at −78 °C using a dry ice-ethanol bath (Fahey et al., 1985). A large excess of O_3 ensured that all the NO_2 was oxidised. O_3 was generated by electrical discharge of O_2, which had been passed through silica gel to remove any residual water vapour.

N_2O_5 was detected using a highly sensitive thermal dissociation cavity-ring-down spectrometer (TD-CRD) as described previously (Schuster et al., 2009; Crowley et al., 2010b). The limit of detection was usually less than about 5 ppt (5 s sampling time). A counter-flow based gas-particle separation method was deployed in order to minimise entry of particles into the TD-CRD without the use of filters. As shown in Fig. 1, ~ 200 sccm flow (6 SLM – F_H – F_I) was sampled from the flow tube through a 1/8″ Teflon tube, diluted by carrier gas (F_H + F_I) to a total flow of 6 SLM (standard litre per minute), and then pumped through the TD-CRD. A 200 sccm counter flow (F_G) was fed into the annular space between the 1/8″ Teflon tube and a 1/4″ steel tube to prevent particles being sampled. This set-up enabled particle free air (< 1 particle cm^{-3}, measured by a TSI 3010 condensation particle counter) to be sampled. Efficient gas-particle separation was very important because the TD-CRD is very sensitive to aerosol light scattering, and because deposition of dust particles onto the inner wall of the sampling tubing should be avoided to minimize the loss of N_2O_5 during transport to the TD-CRD.

The N_2O_5 concentration in the flow tube is much greater than in the TD-CRD. This arises mainly through the dilution effect of the counter flow but is also caused by adding a large carrier gas flow (F_H+ F_I) to rapidly transport N_2O_5 from the flow tube to the optical cavity of the TD-CRD. The overall dilution factor (645) was experimentally determined by introducing a known amount of NO_2 into the flow tube through the injector and measuring its post-dilution concentration at 662 nm by the TD-CRD. NO_2, instead of N_2O_5, was used to determine the dilution effect because its losses through the flow tube are negligible. As NO_2 and N_2O_5 have different diffusion coefficients, they will be differently diluted in the counter-flow, which adds uncertainty (estimated as not more than ~20 %) to the dilution factor. However, as the uptake kinetics is determined by the relative change of N_2O_5 concentrations, and we show that the uptake coefficients are in any case not dependent on the initial N_2O_5 concentration, this is not significant.

3 Results

Two typical datasets showing the response of the N_2O_5 mixing ratio (in parts per trillion, pptv, where 1 pptv $\sim 2.5 \times 10^7$ molecule cm^{-3} at STP) to the introduction of illite and ATD aerosols into the flow tube are displayed in Fig. 3. The obvious anti-correlation between the N_2O_5 mixing ratio (measured by the CRD) and the aerosol number concentration (measured by the APS) indicates substantial interaction between N_2O_5 and the illite/ATD particles. A cursory inspection of the data shows that even short spikes in the dust concentration are accompanied by reductions in N_2O_5 of similar duration. This indicates that, under the operating conditions used, the flow tube is in sufficiently rapid steady state to deliver accurate uptake coefficients.

Figure 3 also shows that when the dust aerosol number concentration returned to 0 particles cm^{-3} after the dust was switched out of the reactor (after ~500–550 s in Fig. 3), the measured N_2O_5 level recovered to the initial value. This indicates that the gas-particle separation was efficient and there was no additional loss of N_2O_5 caused by dust particles being progressively deposited onto the inner wall of the sampling tubing during the experiment.

When the number of reactive sites on the dust surface does not change significantly during the reaction time, the loss of N_2O_5 in the flow tube can be described by

$$[N_2O_5]_t = [N_2O_5]_0 \cdot \exp[-(k_w + k_d) \cdot t] \qquad (2)$$

$$k_d = 0.25\gamma_{exp}\bar{c}N_dA_d \qquad (3)$$

ACPD
13, 24855–24884, 2013
Heterogeneous reaction of N_2O_5
M. J. Tang et al.

where $[N_2O_5]_t$ and $[N_2O_5]_0$ are the measured N_2O_5 mixing ratios at the interaction time (of N_2O_5 with dust aerosols) of 0 and t(s), respectively, k_w is the pseudo-first-order loss rate constant of N_2O_5 onto the wall of the flow tube (s^{-1}), k_d is the pseudo-first-order loss rate constant of N_2O_5 onto dust particle surface (s^{-1}), γ_{exp} is the effective (or experimentally measured) uptake coefficient of N_2O_5 onto dust particles, $\bar{c}$ is the average molecular speed of N_2O_5 (24 096 cm s^{-1} at 296 K), N_d is the dust aerosol number concentration (particle cm^{-3}), and A_d is the average surface area of dust particles (cm^2 per particle).

Uptake experiments were conducted by introducing bursts of dust aerosol (usually around 5–10 min in duration) into the flow tube at 5–6 different injector positions. Equations (2) and (3) suggest that, at each fixed contact time t, i.e. at each fixed injector position, the measured N_2O_5 concentration, $[N_2O_5]_t$, should show an exponential dependence on the aerosol number concentration, N_d, if the wall loss rate (k_w) does not change during the experiment. The experimental dataset displayed in Fig. 4, plotting the measured N_2O_5 concentrations versus the dust aerosol number concentration for both illite and ATD particles at three different injector positions, is consistent with this.

According to Eqs. (2) and (3) The slopes of such plots, $0.25\gamma_{exp}\bar{c}N_dA_dt$, depends linearly on the contact time, t. Typical results for ATD and illite particles, confirming the expected linear relation, are displayed in Fig. 5. Here, the slope is equal to $0.25\gamma_{exp}\bar{c}A_d$ which can be used to derive the effective uptake coefficient (γ_{exp}) when combined with A_d from the aerosol size distribution measured by the APS. Figure 5 shows that at 0 % RH the value of $0.25\gamma_{exp}\bar{c}A_d$ for illite is similar to that for ATD; however, the average surface area of ATD particles is much larger than that of illite particles, suggesting that the uptake of N_2O_5 onto illite particles is more efficient. The non-zero intercept (~ 5 s) in Fig. 5, is the result of non-instantaneous mixing of main-flow and injector flows in the AFT (see above).

The rate of uptake of a trace gas onto aerosol particles is reduced by the concentration gradient close to the particle surface, resulting in an underestimation of the true uptake coefficient, γ. This effect can be corrected by using the following expression

(Fuchs and Sutugin, 1970):

$$\frac{1}{\gamma} = \frac{1}{\gamma_{\rm exp}} - \frac{0.75 + 0.286Kn}{Kn \cdot (Kn + 1)} \quad (4)$$

where Kn is the Knudsen number. For mono-dispersed particles, Kn is given by

$$Kn = \frac{3D(N_2O_5)}{c(N_2O_5) \cdot r} \quad (5)$$

where r is the radius of the particle (cm) and $D(N_2O_5)$ is the gas phase diffusion coefficient of N_2O_5 (0.085 $cm^2\,s^{-1}$ at 296 K). The aerosol particles used in this study are not mono-dispersed and Kn was calculated by

$$Kn = \frac{\sum(N_i \cdot Kn(i))}{\sum N_i} = \frac{3D(N_2O_5)}{c(N_2O_5)} \frac{\sum(N_i/r_i)}{\sum N_i} \quad (6)$$

where N_i and $Kn(i)$ are the aerosol number concentration and the Knudsen number in the i-th size bin with the radius of r_i, respectively.

The heterogeneous reaction of N_2O_5 with illite aerosol particles was investigated at five different relative humidities with initial N_2O_5 concentrations in the range of (11–21) $\times 10^{12}$ molecule cm^{-3}. This is the first time that the heterogeneous interaction of N_2O_5 with illite has been investigated. As shown in the lower panel of Fig. 6, $\gamma(N_2O_5)$ onto illite particles was determined to be $(9.1 \pm 3.9) \times 10^{-2}$, $(9.3 \pm 0.8) \times 10^{-2}$, $(7.2 \pm 2.1) \times 10^{-2}$, $(4.9 \pm 0.6) \times 10^{-2}$, and $(3.9 \pm 1.2) \times 10^{-2}$, when the RH was 0 %, 27 %, 33 %, 50 %, and 67 %, respectively. The diffusion correction factor, defined as $(\gamma - \gamma_{\rm exp})/\gamma_{\rm exp}$, is ~ 20 % at high RH and up to ~ 40 % at low RH owing to the larger uptake coefficient.

The uptake of N_2O_5 onto airborne ATD particles was examined at five different relative humidities (RH) with initial N_2O_5 concentrations in the range of (8–24) $\times 10^{12}$ molecule cm^{-3}. No dependence of $\gamma(N_2O_5)$ on the initial N_2O_5 concentration was found, consistent with the previous aerosol flow tube study of the uptake of

N_2O_5 onto ATD particles (Wagner et al., 2009). The result is summarized in Table 1 and shown in Fig. 6 (upper panel). Our study suggests that $\gamma(N_2O_5)$ onto ATD particles is at most only weakly dependent on RH (0–67 %), and the dataset may be described with an average, RH independent value of $(6.3 \pm 1.6) \times 10^{-3}$ (1σ). The diffusion correction factor is only ~5 % due to the relatively inefficient uptake of N_2O_5 onto ATD particles.

4 Discussion

Very large uptake coefficients were observed for illite, which decreased by a factor of 2–3 as RH was increased from 0 to 67 %. Figure 6 also shows the water adsorption isotherm of illite (lower panel, red curve, right y axis) reported by Hatch et al. (2012). One possible explanation for the decrease in $\gamma(N_2O_5)$ with increasing RH is the competitive adsorption between H_2O and N_2O_5, whereby the increased coverage of H_2O at high RH may result in blocking of particularly reactive surface sites, which are then unavailable for N_2O_5 uptake, yet have insufficient water to support solvation/ionization of N_2O_5 to NO_2^+ and NO_3^-. In this regard, we note that illite, with the general formula: $M_x[Si_{6.8}Al_{1.12}]Al_3Fe_{0.25}Mg_{0.75}O_{20}(OH)_4$ (Hatch et al., 2012), has four OH groups in each structure unit. Previous experimental and theoretical work has shown that N_2O_5 reaction on mineral surfaces is partially controlled by the availability of surface OH groups. Seisel et al. (2005) showed that, for Saharan dust, the infrared absorption of surface OH groups at 3756 cm^{-1} and 3725 cm^{-1} decreased with exposure to N_2O_5 and concluded that the reaction proceeds via two parallel processes: Reaction with the OH groups on the mineral dust surface and the heterogeneous hydrolysis of N_2O_5 by surface adsorbed water.

Using density functional theory to investigate the reactivity of N_2O_5 with $(Si(OH)_4)_2$ (a simplified model of a silica surface) Messaoudi et al. (2013) concluded that surface reaction of N_2O_5 with OH groups on the silica surface is more favorable than its hydrolysis. If similar mechanisms also operate for illite, an increase of RH will lead to "deactivation" of surface OH groups by adsorbed surface water and consequently a decrease of the overall surface reactivity towards N_2O_5.

In this respect it is interesting to note that at 67 % RH, the value of the uptake coefficient (~ 0.04) is similar to $\gamma(N_2O_5)$ onto liquid water surface within the experimental uncertainties (Ammann et al., 2013). This may indicate that at higher RH the heterogeneous surface hydrolysis contributes significantly to the uptake of N_2O_5 whilst at lower RH the more rapid reaction with surface OH groups dominates. The loss of surface reactivity of mineral dust at increasing RH has been previously observed for other trace gases, e.g. H_2O_2 (Pradhan et al., 2010) and O_3 (Mogili et al., 2006b; Nicolas et al., 2009).

The results for ATD reveal a rather different picture, with lower uptake coefficients (factor ~ 10 lower than illite at 0 % RH) and (at most) a weak dependence on RH. The lower uptake coefficients may be related to the mineral composition of ATD which mainly consist of feldspar and quartz (Broadley et al., 2012), which do not have intrinsic surface OH groups. The weak dependence on RH is probably related to the fact that the hygroscopic growth of ATD particles is very small (Gustafsson et al., 2005; Vlasenko et al., 2005) and therefore even at high RH, the amount of adsorbed water on the surface does not contribute significantly to N_2O_5 solvation.

Results from previous studies of the heterogeneous reaction of N_2O_5 with airborne mineral dust particles are compiled in Fig. 7. Values of $\gamma(N_2O_5)$ reported by Knudsen-cell studies (Karagulian et al., 2006; Wagner et al., 2008) are significantly larger than that measured in this work, presumably the result of using bulk samples and the geometric area of the sample holders to calculate the uptake coefficients, which are then upper limits. The drawbacks of using bulk samples in investigation of heterogeneous reactions have been documented previously (Crowley et al., 2010a) and results from bulks samples are not considered further here.

The two sets of uptake coefficients for Saharan dust reported by this group (Wagner et al., 2008; Tang et al., 2012) differ by about a factor of two and display a different dependence on relative humidity. Reasons for this, related to the inferior detection and sampling scheme used in the earlier study, are discussed by Tang et al. (2012).

Figure 7 shows that the uptake coefficients measured for illite in this study are the largest to date followed by Saharan dust (SDCV). The difference between uptake coefficients for illite and Saharan dust is especially significant at low humidity and may be related to the presence of reactive, surface-OH groups on illite as discussed above. The lowest uptake coefficients are observed for dry samples of ATD and calcite. For ATD our results agree well with those reported by Wagner et al. (2009), in which an aerosol flow tube with similar flow conditions as this study was used. The present study extended the RH range investigated to 67 % and confirms the weak trend in $\gamma(N_2O_5)$ (slightly negative) with increasing RH.

Figure 7 highlights the importance of studing heterogeneous reactions of N_2O_5 on mineral dust at atmospherically relevant relative humidities as different minerals or mineral dust components display different behavior. Indeed, while $CaCO_3$ is the least reactive at low humidity, the uptake coefficient of N_2O_5 at RH close to 70 % is similar for both $CaCO_3$ and Saharan dust, and only slightly lower than for illite (which displays the opposite trend with RH as described above). The significant increase of $\gamma(N_2O_5)$ onto $CaCO_3$ at high RH bears resemblance to its water adsorption isotherm (Gustafsson et al., 2005) and is likely to be related to the formation of more reactive $Ca(OH)(CO_3H)$ on the surface at higher RH (Al-Hosney et al., 2005).

The lack of RH dependence of $\gamma(N_2O_5)$ onto Saharan dust particles is potentailly related to the fact that Saharan dust is a complex mixture of different minerals which have different heterogeneous reactivity towards N_2O_5, which may also vary both in positive or negative sense with increasing RH. We note that the reactivity of N_2O_5 on illite and Saharan dust particles tends to a common value at high RH, suggesting that at under these conditions heterogeneous hydrolysis drives the N_2O_5 uptake onto clay minerals. Indeed, the uptake coefficients at high RH are similar in magnitude to that of N_2O_5 onto aqueous solutions (Ammann et al., 2013).

ACPD
13, 24855–24884, 2013

Further kinetics and mechanistic investigations of the effect of relative humidity on the uptake of N_2O_5 onto other important minerals present in dust particles, e.g. kaolinite and feldspars, will help to improve our understanding the heterogeneous reaction of N_2O_5 with mineral dust particles and allow us to transfer laboratory derived uptake coefficients to the atmsphere with more confidence. The present database (Crowley et al., 2010a) on the uptake of N_2O_5 (and indeed most trace gases) to mineral aerosol is too incomplete to enable accurate, mineralogically distinct (or dust source region dependent) global modelling of the effects of N_2O_5 uptake to dust particles. As long as this situation persists, average uptake coefficients, derived from experiments on Saharan dust samples may represent the best alternative. Arizona dust is unlikely to be a useful alternative in this regard.

5 Conclusions

The heterogeneous interaction of N_2O_5 with illite and Arizona Test Dust (ATD) particles was investigated using an aerosol flow tube at room temperature and different relative humidities (up to 67 %). For illite, the uptake coefficient was found to be very large and to decrease from $(9.1 \pm 3.9) \times 10^{-2}$ at 0 % RH to $(3.9 \pm 1.2) \times 10^{-2}$ at 67 % RH. Much lower uptake coefficients, $(6.3 \pm 1.6) \times 10^{-3}$ (1σ), and a significantly weaker dependence on RH was found for ATD. Whilst the uptake coefficients for interaction of N_2O_5 with illite calcite and Saharan dust tend to a common value of ≈ 0.03 at high relative humidities, the much weaker interaction of N_2O_5 with ATD ($\gamma \sim 0.004$ at similar RH) may indicate that its common usage as a laboratory surrogate for atmospheric mineral dust may not necessarily lead to conclusions that can be applied with confidence to the mineralogically distinct “global mineral dust” which is dominated by emissions from the Saharan and Asian desserts.

Acknowledgements. This work was financed by the International Max-Planck-Research school at the MPI in Mainz and the Deutsche Forschungs Gemeinschaft (DFG-INSU/CNRS, “Atmochem – CR246/1-1”). We gratefully acknowledge Du Pont (Switzerland) for providing the

FEP suspension used to coat the cavity walls of the CRD instrument.

The service charges for this open access publication have been covered by the Max Planck Society.

References

Al-Hosney, H. A., Carlos-Cuellar, S., Baltrusaitis, J., and Grassian, V. H.: Heterogeneous uptake and reactivity of formic acid on calcium carbonate particles: a Knudsen cell reactor, FTIR and SEM study, Phys. Chem. Chem. Phys., 7, 3587–3595, 2005.

Ammann, M., Cox, R. A., Crowley, J. N., Jenkin, M. E., Mellouki, A., Rossi, M. J., Troe, J., and Wallington, T. J.: Evaluated kinetic and photochemical data for atmospheric chemistry: Volume VI–heterogeneous reactions with liquid substrates, Atmos. Chem. Phys., 13, 8045–8228, doi:10.5194/acp-13-8045-2013, 2013.

Balkanski, Y., Schulz, M., Claquin, T., and Guibert, S.: Reevaluation of Mineral aerosol radiative forcings suggests a better agreement with satellite and AERONET data, Atmos. Chem. Phys., 7, 81–95, doi:10.5194/acp-7-81-2007, 2007.

Broadley, S. L., Murray, B. J., Herbert, R. J., Atkinson, J. D., Dobbie, S., Malkin, T. L., Condliffe, E., and Neve, L.: Immersion mode heterogeneous ice nucleation by an illite rich powder representative of atmospheric mineral dust, Atmos. Chem. Phys., 12, 287–307, doi:10.5194/acp-12-287-2012, 2012.

Brown, S. S., Ryerson, T. B., Wollny, A. G., Brock, C. A., Peltier, R., Sullivan, A. P., Weber, R. J., Dube, W. P., Trainer, M., Meagher, J. F., Fehsenfeld, F. C., and Ravishankara, A. R.: Variability in nocturnal nitrogen oxide processing and its role in regional air quality, Science, 311, 67–70, 2006.

Chester, R.: The atmospheric transport of clay minerals to the world ocean, Sci. Géol. Mém., 88, 23–32, 1990.

Claquin, T., Schulz, M., and Balkanski, Y. J.: Modeling the mineralogy of atmospheric dust sources, J. Geophys. Res.-Atmos., 104, 22243–22256, 1999.

Crowley, J. N., Ammann, M., Cox, R. A., Hynes, R. G., Jenkin, M. E., Mellouki, A., Rossi, M. J., Troe, J., and Wallington, T. J.: Evaluated kinetic and photochemical data for atmospheric

chemistry: Volume V–heterogeneous reactions on solid substrates, Atmos. Chem. Phys., 10, 9059–9223, doi:10.5194/acp-10-9059-2010, 2010a.
Crowley, J. N., Schuster, G., Pouvesle, N., Parchatka, U., Fischer, H., Bonn, B., Bingemer, H., and Lelieveld, J.: Nocturnal nitrogen oxides at a rural mountain-site in south-western Germany, Atmos. Chem. Phys., 10, 2795–2812, doi:10.5194/acp-10-2795-2010, 2010b.
Cziczo, D. J., Froyd, K. D., Gallavardin, S. J., Moehler, O., Benz, S., Saathoff, H., and Murphy, D. M.: Deactivation of ice nuclei due to atmospherically relevant surface coatings, Environ. Res. Lett., 4, doi:10.1088/1748-9326/4/4/044013, 2009.
De Reus, M., Fischer, H., Sander, R., Gros, V., Kormann, R., Salisbury, G., Van Dingenen, R., Williams, J., Zöllner, M., and Lelieveld, J.: Observations and model calculations of trace gas scavenging in a dense Saharan dust plume during MINATROC, Atmos. Chem. Phys., 5, 1787–1803, doi:10.5194/acp-5-1787-2005, 2005.
DeMott, P. J., Sassen, K., Poellot, M. R., Baumgardner, D., Rogers, D. C., Brooks, S. D., Prenni, A. J., and Kreidenweis, S. M.: African dust aerosols as atmospheric ice nuclei, Geophys. Res. Lett., 30, L07808, doi:10.1029/2009GL037639, 2003.
Dentener, F. J. and Crutzen, P. J.: Reaction of N_2O_5 on tropospheric aerosols – Impact on the global distributions of NO_x, O_3, and OH, J. Geophys. Res.-Atmos., 98, 7149–7163, 1993.
Dentener, F. J., Carmichael, G. R., Zhang, Y., Lelieveld, J., and Crutzen, P. J.: Role of mineral aerosol as a reactive surface in the global troposphere, J. Geophys. Res.-Atmos., 101, 22869–22889, 1996.
Eastwood, M. L., Cremel, S., Gehrke, C., Girard, E., and Bertram, A. K.: Ice nucleation on mineral dust particles: Onset conditions, nucleation rates and contact angles, J. Geophys. Res.-Atmos., 113, D22203, doi:10.1029/2008jd010639, 2008.
Evans, M. J. and Jacob, D. J.: Impact of new laboratory studies of N_2O_5 hydrolysis on global model budgets of tropospheric nitrogen oxides, ozone, and OH, Geophys. Res. Lett., 32, L09813, doi:10.1029/2005GL022469, 2005.
Fahey, D. W., Eubank, C. S., Hubler, G., and Fehsenfeld, F. C.: A Calibrated Source of N_2O_5, Atmos. Environ., 19, 1883–1890, 1985.
Fairlie, T. D., Jacob, D. J., Dibb, J. E., Alexander, B., Avery, M. A., van Donkelaar, A., and Zhang, L.: Impact of mineral dust on nitrate, sulfate, and ozone in transpacific Asian pollution plumes, Atmos. Chem. Phys., 10, 3999–4012, doi:10.5194/acp-10-3999-2010, 2010.
Fuchs, N. A. and Sutugin, A. G.: Highly dispersed aerosols, Ann Arbor Sci., Ann Arbor, chapter 3, 46 pp., 1970.

ACPD
13, 24855–24884, 2013

Heterogeneous reaction of N_2O_5

M. J. Tang et al.

Gustafsson, R. J., Orlov, A., Badger, C. L., Griffiths, P. T., Cox, R. A., and Lambert, R. M.: A comprehensive evaluation of water uptake on atmospherically relevant mineral surfaces: DRIFT spectroscopy, thermogravimetric analysis and aerosol growth measurements, Atmos. Chem. Phys., 5, 3415–3421, doi:10.5194/acp-5-3415-2005, 2005.

Hatch, C. D., Wiese, J. S., Crane, C. C., Harris, K. J., Kloss, H. G., and Baltrusaitis, J.: Water Adsorption on Clay Minerals As a Function of Relative Humidity: Application of BET and Freundlich Adsorption Models, Langmuir, 28, 1790–1803, doi:10.1021/la2042873, 2012.

Hinds, W. C.: Aerosol techniques: properties, behavior, and measurement of airborne particles, John Wiley& Sons. Inc., New York, 1996.

Kanji, Z. A., Welti, A., Chou, C., Stetzer, O., and Lohmann, U.: Laboratory studies of immersion and deposition mode ice nucleation of ozone aged mineral dust particles, Atmos. Chem. Phys., 13, 9097–9118, doi:10.5194/acp-13-9097-2013, 2013.

Karagulian, F., Santschi, C., and Rossi, M. J.: The heterogeneous chemical kinetics of N2O5 on CaCO3 and other atmospheric mineral dust surrogates, Atmos. Chem. Phys., 6, 1373–1388, doi:10.5194/acp-6-1373-2006, 2006.

Keyser, L. F.: High-pressure flow kinetics- A study of the OH + HCl reaction from 2 to 100 Torr, J. Phys. Chem., 88, 4750–4758, doi:10.1021/j150664a061, 1984.

Klein, H., Nickovic, S., Haunold, W., Bundke, U., Nillius, B., Ebert, M., Weinbruch, S., Schuetz, L., Levin, Z., Barrie, L. A., and Bingemer, H.: Saharan dust and ice nuclei over Central Europe, Atmos. Chem. Phys., 10, 10211–10221, doi:10.5194/acp-10-10211-2010, 2010.

Krueger, B. J., Grassian, V. H., Laskin, A., and Cowin, J. P.: The transformation of solid atmospheric particles into liquid droplets through heterogeneous chemistry: Laboratory insights into the processing of calcium containing mineral dust aerosol in the troposphere, Geophys. Res. Lett., 30, 1148, doi:10.1029/2002GL016563, 2003.

Laskin, A., Iedema, M. J., Ichkovich, A., Graber, E. R., Taraniuk, I., and Rudich, Y.: Direct observation of completely processed calcium carbonate dust particles, Faraday Disc., 130, 453–468, doi:10.1039/b417366j, 2005.

Macintyre, H. L. and Evans, M. J.: Sensitivity of a global model to the uptake of N2O5 by tropospheric aerosol, Atmos. Chem. Phys., 10, 7409–7414, doi:10.5194/acp-10-7409-2010, 2010

Matsuki, A., Iwasaka, Y., Shi, G. Y., Zhang, D. Z., Trochkine, D., Yamada, M., Kim, Y. S., Chen, B., Nagatani, T., Miyazawa, T., Nagatani, M., and Nakata, H.: Morphological and chemical modification of mineral dust: Observational insight into the heterogeneous uptake of acidic gases, Geophys. Res. Lett., 32, L22806, doi:10.1029/2005GL0244176, 2005.

Messaoudi, S., Bejaoui, B., Akrout, F., Hassen, M. B., and Sammari, C.: Exploration of the reactivity of N_2O_5 with two $Si(OH)_4$ monomers using electronic structure methods, Int. J. Quantum Chem., 113, 1633–1640, doi:10.1002/qua.24378, 2013.

Mogili, P. K., Kleiber, P. D., Young, M. A., and Grassian, V. H.: N_2O_5 hydrolysis on the components of mineral dust and sea salt aerosol: Comparison study in an environmental aerosol reaction chamber, Atmos. Environ., 40, 7401–7408, 2006a.

Mogili, P. K., Kleiber, P. D., Young, M. A., and Grassian, V. H.: Heterogeneous uptake of ozone on reactive components of mineral dust aerosol: An environmental aerosol reaction chamber study, J. Phys. Chem. A, 110, 13799–13807, 2006b.

Mori, I., Nishikawa, M., Tanimura, T., and Quan, H.: Change in size distribution and chemical composition of kosa (Asian dust) aerosol during long-range transport, Atmos. Environ., 37, 4253–4263, 2003.

Nickovic, S., Vukovic, A., Vujadinovic, M., Djurdjevic, V., and Pejanovic, G.: Technical Note: High-resolution mineralogical database of dust-productive soils for atmospheric dust modeling, Atmos. Chem. Phys., 12, 845–855, doi:10.5194/acp-12-845-2012, 2012.

Nicolas, M., Ndour, M., Ka, O., D'Anna, B., and George, C.: Photochemistry of Atmospheric Dust: Ozone Decomposition on Illuminated Titanium Dioxide, Env. Sci. Tech., 43, 7437–7442, doi:10.1021/es901569d, 2009.

Niedermeier, D., Hartmann, S., Shaw, R. A., Covert, D., Mentel, T. F., Schneider, J., Poulain, L., Reitz, P., Spindler, C., Clauss, T., Kiselev, A., Hallbauer, E., Wex, H., Mildenberger, K., and Stratmann, F.: Heterogeneous freezing of droplets with immersed mineral dust particles–measurements and parameterization, Atmos. Chem. Phys., 10, 3601–3614, doi:10.5194/acp-10-3601-2010, 2010.

Osthoff, H. D., Pilling, M. J., Ravishankara, A. R., and Brown, S. S.: Temperature dependence of the NO_3 absorption cross-section above 298 K and determination of the equilibrium constant for $NO_3 + NO_2$ <->N_2O_5 at atmospherically relevant conditions, Phys. Chem. Chem. Phys., 9, 5785–5793, 2007.

Osthoff, H. D., Roberts, J. M., Ravishankara, A. R., Williams, E. J., Lerner, B. M., Sommariva, R., Bates, T. S., Coffman, D., Quinn, P. K., Dibb, J. E., Stark, H., Burkholder, J. B., Talukdar, R. K., Meagher, J., Fehsenfeld, F. C., and Brown, S. S.: High levels of nitryl chloride in the polluted subtropical marine boundary layer, Nature Geoscience, 1, 324–328, 2008.

ACPD
13, 24855–24884, 2013

Phillips, G. J., Tang, M. J., Thieser, J., Brickwedde, B., Schuster, G., Bohn, B., Lelieveld, J., and Crowley, J. N.: Significant concentrations of nitryl chloride observed in rural continental Europe associated with the influence of sea salt chloride and anthropogenic emissions, Geophys. Res. Lett., 39, L10811, doi:10.1029/2012GL051912, 2012.

Pradhan, M., Kalberer, M., Griffiths, P. T., Braban, C. F., Pope, F. D., Cox, R. A., and Lambert, R. M.: Uptake of Gaseous Hydrogen Peroxide by Submicrometer Titanium Dioxide Aerosol as a Function of Relative Humidity, Env. Sci. Tech., 44, 1360–1365, doi:10.1021/es902916f, 2010.

Prospero, J. M.: Long-range transport of mineral dust in the global atmosphere: Impact of African dust on the environment of the southeastern United States, P. Natl. Acad. Sci. USA, 96, 3396–3403, 1999.

Schuster, G., Labazan, I., and Crowley, J. N.: A cavity ring down/cavity enhanced absorption device for measurement of ambient NO_3 and N_2O_5, Atmos. Meas. Tech., 2, 1–13, doi:10.5194/amt-2-1-2009, 2009.

Schuttlefield, J. D., Cox, D., and Grassian, V. H.: An investigation of water uptake on clays minerals using ATR-FTIR spectroscopy coupled with quartz crystal microbalance measurements, J. Geophys. Res.-Atmos., 112, L22806, doi:10.1029/2007jd008973, 2007.

Seisel, S., Börensen, C., Vogt, R., and Zellner, R.: Kinetics and mechanism of the uptake of N_2O_5 on mineral dust at 298 K, Atmos. Chem. Phys., 5, 3423–3432, doi:10.5194/acp-5-3423-2005, 2005.

Shi, Z., Zhang, D., Hayashi, M., Ogata, H., Ji, H., and Fujiie, W.: Influences of sulfate and nitrate on the hygroscopic behaviour of coarse dust particles, Atmos. Environ., 42, 822–827, doi:10.1016/j.atmosenv.2007.10.037, 2008.

Sullivan, R. C., Guazzotti, S. A., Sodeman, D. A., and Prather, K. A.: Direct observations of the atmospheric processing of Asian mineral dust, Atmos. Chem. Phys., 7, 1213–1236, doi:10.5194/acp-7-1213-2007, 2007.

Sullivan, R. C., Moore, M. J. K., Petters, M. D., Kreidenweis, S. M., Roberts, G. C., and Prather, K. A.: Timescale for hygroscopic conversion of calcite mineral particles through heterogeneous reaction with nitric acid, Phys. Chem. Chem. Phys., 11, 7826–7837, doi:10.1039/b904217b, 2009.

Sullivan, R. C., Minambres, L., DeMott, P. J., Prenni, A. J., Carrico, C. M., Levin, E. J. T., and Kreidenweis, S. M.: Chemical processing does not always impair heterogeneous ice nucle-

ation of mineral dust particles, Geophys. Res. Lett., 37, L24805, doi:10.1029/2010gl045540, 2010.
Tang, M. J., Thieser, J., Schuster, G., and Crowley, J. N.: Kinetics and mechanism of the heterogeneous reaction of N_2O_5 with mineral dust particles, Phys. Chem. Chem. Phys., 14, 8551–8561, 2012.
Textor, C., Schulz, M., Guibert, S., Kinne, S., Balkanski, Y., Bauer, S., Berntsen, T., Berglen, T., Boucher, O., Chin, M., Dentener, F., Diehl, T., Easter, R., Feichter, H., Fillmore, D., Ghan, S., Ginoux, P., Gong, S., Grini, A., Hendricks, J., Horowitz, L., Huang, P., Isaksen, I., Iversen, I., Kloster, S., Koch, D., Kirkevåg, A., Kristjansson, J. E., Krol, M., Lauer, A., Lamarque, J. F., Liu, X., Montanaro, V., Myhre, G., Penner, J., Pitari, G., Reddy, S., Seland, ø., Stier, P., Takemura, T., and Tie, X.: Analysis and quantification of the diversities of aerosol life cycles within AeroCom, Atmos. Chem. Phys., 6, 1777–1813, doi:10.5194/acp-6-1777-2006, 2006
Thornton, J. A., Kercher, J. P., Riedel, T. P., Wagner, N. L., Cozic, J., Holloway, J. S., Dube, W. P., Wolfe, G. M., Quinn, P. K., Middlebrook, A. M., Alexander, B., and Brown, S. S.: A large atomic chlorine source inferred from mid-continental reactive nitrogen chemistry, Nature, 464, 271–274, doi:10.1038/nature08905, 2010.
Tobo, Y., Zhang, D. Z., Matsuki, A., and Iwasaka, Y.: Asian dust particles converted into aqueous droplets under remote marine atmospheric conditions, P. Natl. Acad. Sci. USA, 107, 17905–17910, doi:10.1073/pnas.1008235107, 2010.
Twohy, C. H., Kreidenweis, S. M., Eidhammer, T., Browell, E. V., Heymsfield, A. J., Bansemer, A. R., Anderson, B. E., Chen, G., Ismail, S., DeMott, P. J., and Van den Heever, S. C.: Saharan dust particles nucleate droplets in eastern Atlantic clouds, Geophys. Res. Lett., 36, L01807, doi:10.1029/2008gl035846, 2009.
Vlasenko, A., Sjogren, S., Weingartner, E., Gaggeler, H. W., and Ammann, M.: Generation of submicron Arizona test dust aerosol: Chemical and hygroscopic properties, Aerosol Sci. Tech., 39, 452–460, 2005.
Wagner, C., Hanisch, F., Holmes, N., de Coninck, H., Schuster, G., and Crowley, J. N.: The interaction of N2O5 with mineral dust: aerosol flow tube and Knudsen reactor studies, Atmos. Chem. Phys., 8, 91–109, doi:10.5194/acp-8-91-2008, 2008.
Wagner, C., Schuster, G., and Crowley, J. N.: An aerosol flow tube study of the interaction of N_2O_5 with calcite, Arizona dust and quartz, Atmos. Environ., 43, 5001–5008, 2009.
Wang, K., Zhang, Y., Nenes, A., and Fountoukis, C.: Implementation of dust emission and chemistry into the Community Multiscale Air Quality modeling system and initial application

to an Asian dust storm episode, Atmos. Chem. Phys., 12, 10209–10237, doi:10.5194/acp-12-10209-2012, 2012.
Wayne, R. P., Barnes, I., Biggs, P., Burrows, J. P., Canosa-Mas, C. E., Hjorth, J., Le Bras, G., Moortgat, G. K., Perner, D., Poulet, G., Restelli, G., and Sidebottom, H.: The nitrate radical: Physics, chemistry, and the atmosphere, Atmos. Environ. A, 25A, 1–206, 1991.
Zhu, S., Butler, T., Sander, R., Ma, J., and Lawrence, M. G.: Impact of dust on tropospheric chemistry over polluted regions: a case study of the Beijing megacity, Atmos. Chem. Phys., 10, 3855–3873, doi:10.5194/acp-10-3855-2010, 2010.
Zimmermann, F., Weinbruch, S., Schutz, L., Hofmann, H., Ebert, M., Kandler, K., and Worringen, A.: Ice nucleation properties of the most abundant mineral dust phases, J. Geophys. Res.-Atmos., 113, D23204, doi:10.1029/2008jd010655, 2008.

ACPD
13, 24855–24884, 2013

Heterogeneous reaction of N_2O_5

M. J. Tang et al.

Table 1. Uptake coefficients for N_2O_5 on illite and ADT.

$\gamma(N_2O_5)$ ($\times 10^3$)	RH (%)	$[N_2O_5]^*$	Mineral
91 ± 39	0		
93 ± 8	17		
72 ± 21	33	$(8–24) \times 10^{12}$	illite
49 ± 6	50		
39 ± 12	67		
7.7 ± 1.0	0		
6.0 ± 2.0	17		
7.4 ± 0.7	33	$(11–22) \times 10^{12}$	ATD
4.9 ± 1.3	50		
5.0 ± 0.3	67		

* N_2O_5 concentration in units of molecule cm^{-3}.

ACPD
13, 24855–24884, 2013

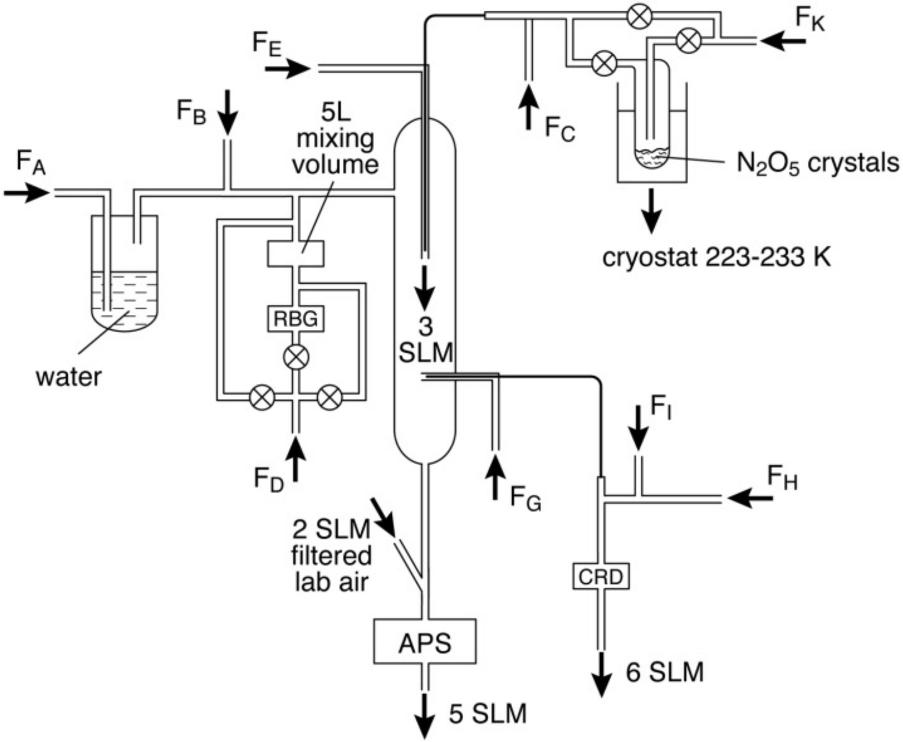

Fig. 1. Schematic diagram of the aerosol flow tube. RBG = Rotating Brush Generator, APS = Aerodynamic Particle Sizer, CRD = Cavity Ring-Down spectrometer.

ACPD
13, 24855–24884, 2013

Title Page
Abstract | Introduction
Conclusions | References
Tables | Figures
◂◂ | ▸▸
◂ | ▸
Back | Close
Full Screen / Esc
Printer-friendly Version
Interactive Discussion

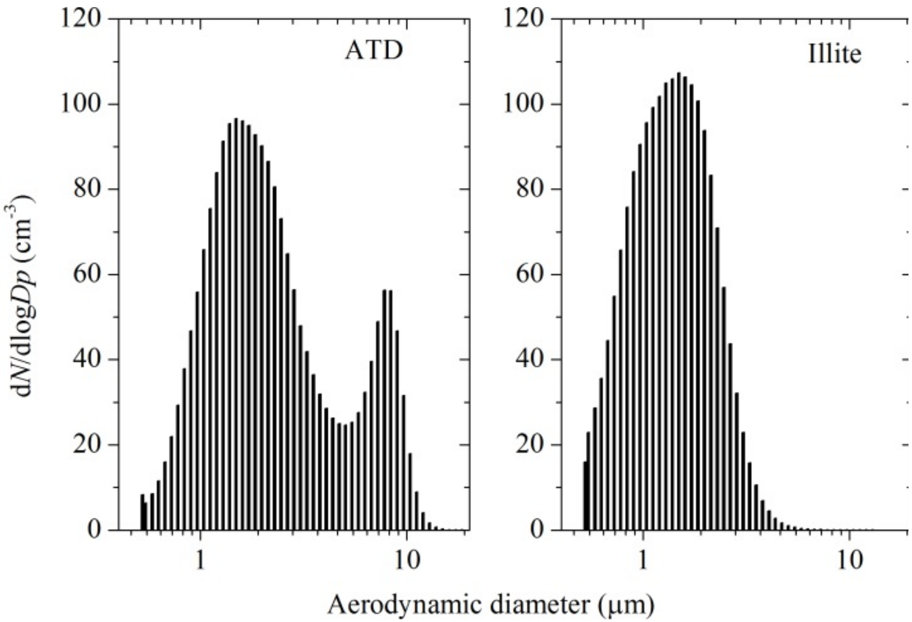

Fig. 2. Typical size distribution of ATD and illite particles measured at the downstream end of the aerosol flow tube.

ACPD
13, 24855–24884, 2013

Heterogeneous reaction of N_2O_5

M. J. Tang et al.

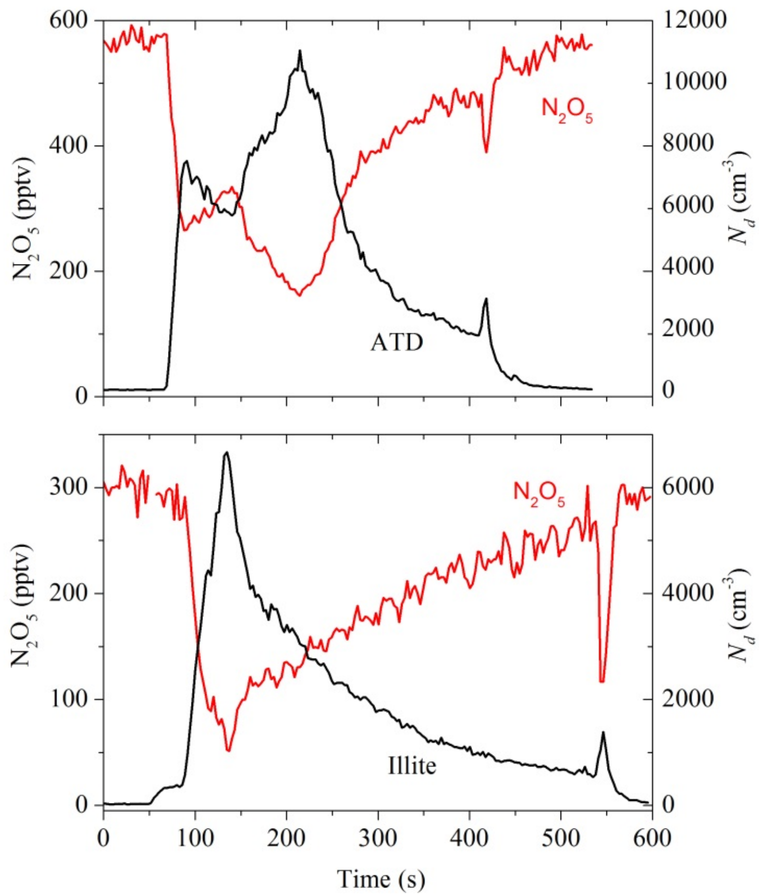

Fig. 3. Response of the N_2O_5 mixing ratio (left axis) to the introduction of mineral dust aerosols (right *y* axis) into the flow tube at RH = 0 % when the injector was at 70 cm. The time between acquisition of neighbouring data points is ∼ 3 s.

ACPD
13, 24855–24884, 2013

Title Page
Abstract | Introduction
Conclusions | References
Tables | Figures
◂I | ▸I
◂ | ▸
Back | Close
Full Screen / Esc
Printer-friendly Version
Interactive Discussion

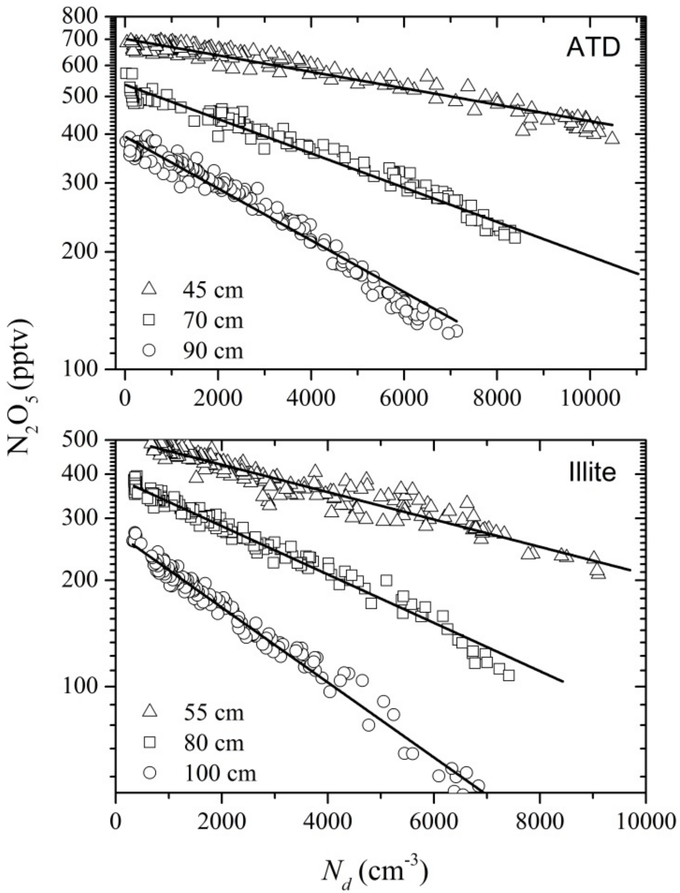

Fig. 4. Exponential dependence of the measured N_2O_5 mixing ratio on the dust aerosol number concentration at three different injector positions at RH = 0 %.

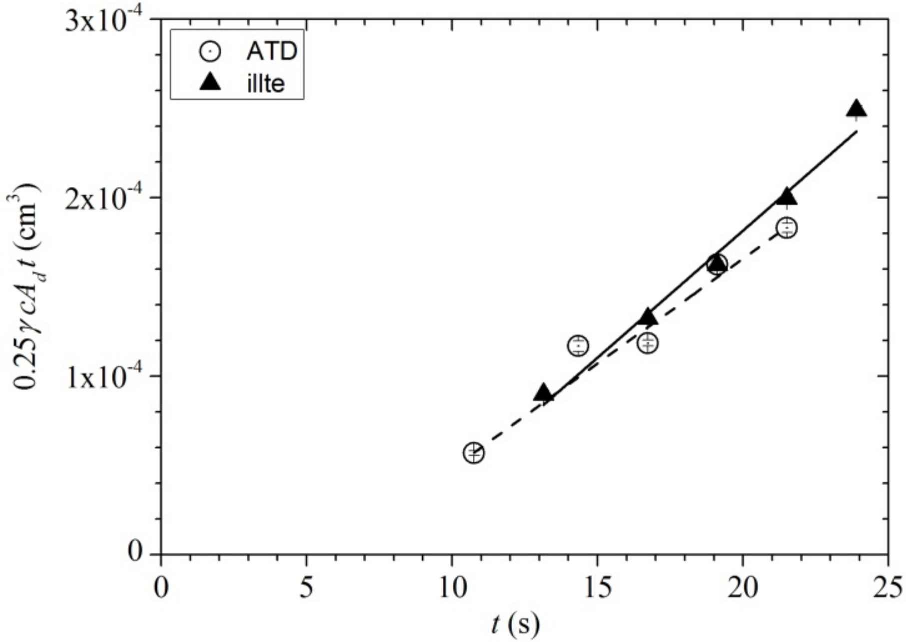

Fig. 5. Plot of $0.25\gamma_{exp}\bar{c}N_d A_d t$, versus the contact time (t) for N_2O_5 with dust aerosols in the AFT. The lines are least-squares fits to the illite (solid line) and ATD (dashed line) datasets. The error bars are statistical (2σ) only.

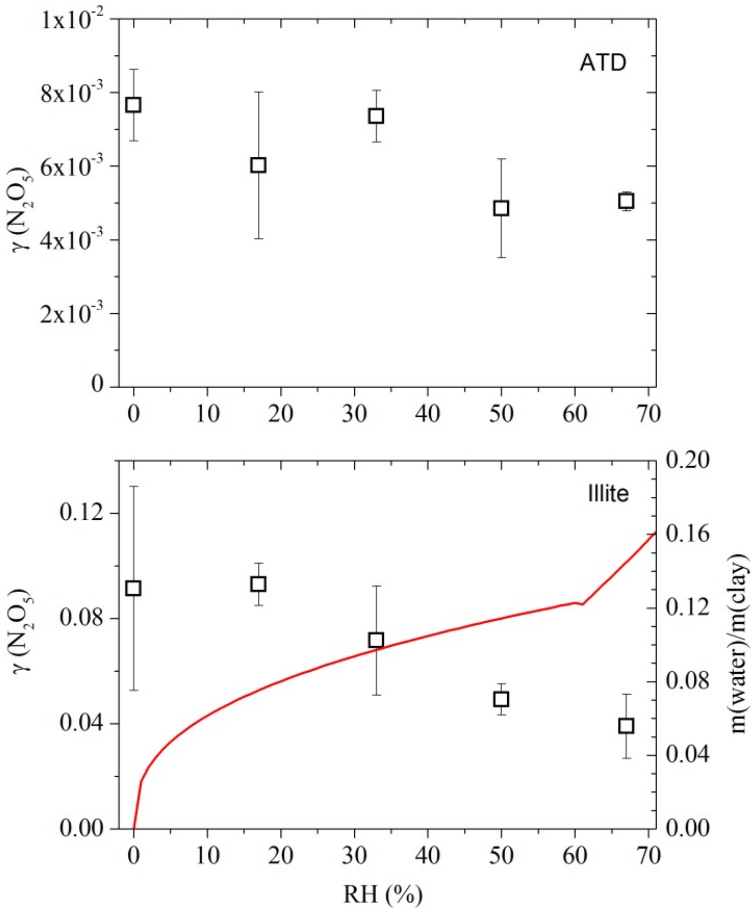

Fig. 6. Uptake coefficients of N_2O_5 at different relative humidities to illite and ATD. The ratio of the mass of absorbed water to that of dry illite (lower panel, red curve, right *y* axis) is also plotted as a function of RH (Hatch et al., 2012).

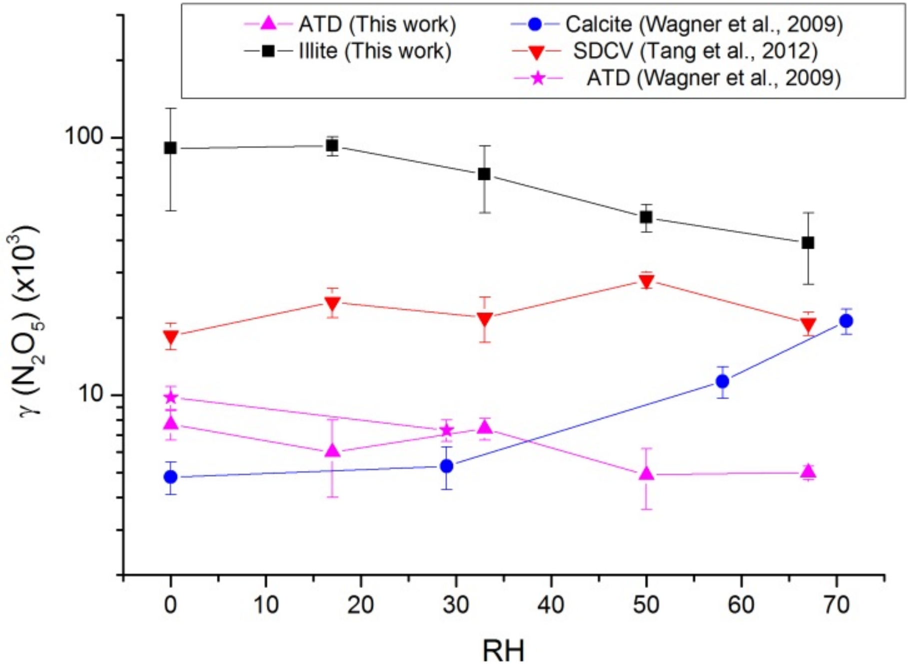

Fig. 7. Comparison of relative humidity dependence of N_2O_5 uptake coefficients to airborne mineral dust particles.

ACPD
13, 24855–24884, 2013